

Equilibrium statistical mechanics on correlated random graphs

Adriano Barra ¹, Elena Agliari ²

¹ Dipartimento di Fisica, Sapienza Università di Roma (Italy)
GNFM Gruppo Nazionale per la Fisica Matematica

² Dipartimento di Fisica, Università di Parma (Italy)
INFN, Gruppo Collegato di Parma (Italy)

Theoretische Polymerphysik, Albert-Ludwigs-Universität, Freiburg (Germany)

Abstract.

Biological and social networks have recently attracted enormous attention between physicists. Among several, two main aspects may be stressed: A non trivial topology of the graph describing the mutual interactions between agents exists and/or, typically, such interactions are essentially (weighted) imitative. Despite such aspects are widely accepted and empirically confirmed, the schemes currently exploited in order to generate the expected topology are based on a-priori assumptions and in most cases still implement constant intensities for links.

Here we propose a simple shift $[-1, +1] \rightarrow [0, +1]$ in the definition of patterns in an Hopfield model to convert frustration into dilution: By varying the bias of the pattern distribution, the network topology -which is generated by the reciprocal affinities among agents (the Hebbian kernel)- crosses various well known regimes (fully connected, linearly diverging connectivity, extreme dilution scenario, no network), coupled with small world properties, which, in this context, are emergent and no longer imposed a-priori.

The model is investigated at first focusing on these topological properties of the emergent network, then its thermodynamics is analytically solved (at a replica symmetric level) by extending the double stochastic stability technique, and presented together with its fluctuation theory for a picture of criticality: both a statistical mechanics and a topological phase diagrams are obtained.

Overall the picture depicted from statistical mechanics is quite intuitive: at least at equilibrium, dilution (of whatever kind) simply decreases the strength of the coupling felt by the spins, but leaves the paramagnetic/ferromagnetic flavors unchanged.

The main difference with respect to previous investigations and a naive picture is that within our approach replicas do not appear: instead of (multi)-overlaps as order parameters, we introduce a class of magnetizations on all the possible sub-graphs belonging to the main one investigated: As a consequence, for these objects a closure for a self-consistent relation is achieved.

¹e-mail:adriano.barra@roma1.infn.it

²e-mail:elena.agliari@fis.unipr.it

1 Introduction to social and biological networks

The paper is organized as follows:

In this section we briefly introduce the reader to the state of the art in the applications of this model to investigation of collective effects in social and biological networks, then, in section 2, we present the model itself with all the related definitions. Section 3 deals with the topological analysis: Techniques from graph theory are the tools. Section 4 deals with the thermodynamical analysis: techniques from statistical mechanics are the tools. In section 5 we present our discussion and outlooks.

Starting with a digression on social sciences, since the early investigations by Milgram [63], several efforts have been made to understand the structure of interactions occurring within a social system. Granovetter defined this field of science as "a tool for linking micro and macro levels of sociological theories" [52] and gave fundamental prescriptions; in particular, he noticed that the stronger the link between two agents and the larger (on average) the overlap among the number of common nearest neighbors, i.e. high degree of cliqueness. Furthermore he noticed that weak ties play a fundamental role acting as bridges among sub-clusters of highly connected interacting agents [52, 53, 54]. As properly pointed out by Watts and Strogatz [71], from a topological viewpoint, the simplest Erdos-Renyi graphs [29] is unable to describe social systems, due to the uncorrelatedness among its links, which constraints the resulting degree of cliqueness to be relatively small [14]. Through a mathematical technique (rewiring), they obtained a first attempt in defining the so called "small world" graph [72]: when trying to implement statistical mechanics on such a topology their network has been essentially seen as a chain of nearest neighbors overlapped on a sparse Erdos-Renyi graph [65, 24]. As the former can be solved via the transfer matrix, the latter via e.g. the replica trick, the model was already understood even from a statistical mechanics perspective (without introducing here a discussion on possible replica symmetry breaking in complex diluted systems [39, 20]).

Coupled to topological investigations, even the analysis of the kind of interactions (still within a "statistical mechanics flavor") started in the past decades in econometrics and, after McFadden described the discrete choice as a one-body theory with external fields [60], Brock and Durlauf went over and gave a clear positive interaction strength to social ties [32, 40].

Even though clearly, as discussed for instance in [21], the role of anti-imitative actions is fundamental for collective decision capabilities, the largest part of interactions is imitative and this prescription will be followed through the paper.

Somewhat close to social breakthrough, after the revolution of Watson and Crick, biological studies in the past fifty years gave rise to completely new field of science as genomics [42], proteomics [46] and metabolic network investigations [59] which ultimately are strongly based on graph theories³ [15]. Furthermore graph structure appears at various levels, i.e. in matching epitopal complementary among antibodies giving rise to the so called "Jerne network" [58][66] for the immune system [18, 1], or at even larger scales of the biological world: from the so far exploited micro and meso, to such a macro as virus spreading worldwide [25], food web [64], and much more [34].

In these contexts, surely there is a disordered underlying structure, but thinking at it as "completely random" is probably a too strong simplifying assumption. One of the strongest starting point when

³It is in fact well established that complex organisms share roughly the same amount of genes with simpler ones. As a result the failure of a purely reductionism approach (more genes \rightarrow more complexity) seems raising and interest in their connections, their network of exchanges, is enormously increasing.

dealing with random coupling is their independence: for example Blake pointed out [28] that exons in haemoglobin correspond both to structural and functional units of protein, implicitly suggesting a not null level of correlation among the "randomness" we have to deal with when trying a statistical mechanics approach. Not too different is the viewpoint of Coolen and coworkers [38][70].

From a completely different background, last step in this introduction is presenting the Hopfield model [56], which, instead, is the paradigmatic model for neural networks. Even though apparently far from topology investigations, in the Hopfield model there is a scalar product among the bit strings (the Hebbian kernel [55]): despite fully connected, the latter can be seen as a measure of the strength of the ties (which in that context must be both positive and negative as, in order to share statically memories over all neurons [10], it must use properties of spin glasses [17][22][62] as the key for having several minima in the fitness landscape). By varying tunable parameters (level of noise and amount of storage memories) the Hopfield model displays a region where is paramagnetic, a region where is a spin glass and a region where is a "working memory" [11][12].

We are ready to introduce our starting idea: what happens if instead of using positive and negative values for the coupling in the Hebbian kernel of the Hopfield model, we use positive and null values?

We want to show that, even in this context, by varying the tunable parameters, we recover several topologies (on which ferromagnetic or paramagnetic behaviors may arise): fully connected scenario weighted and un-weighted, Erdős-Rényi graphs, linearly diverging connectivity, extreme dilutions, small world features, fully disconnected (that is no edges at all).

Despite a rich plethora of phenomena in graph theory is obtained, from equilibrium statistical mechanics perspective we find that all these networks behave not drastically differently, relating strong differences in dynamical features (in agreement with intuition), on which we plan to investigate soon.

2 The model: Definitions

Let us consider V agents $\pm 1 \ni \sigma_i, i \in (1, \dots, V)$. In social framework (e.g. discrete choice in econometrics) for example $\sigma_i = +1$ means that the i^{th} agent agrees a particular choice (and obviously disagreement in the -1 case). In biological networks, i may label a Kauffman gene (assuming undirected links) or a Jerne lymphocytes in such a way that $\sigma_i = +1$ represents expression or firing state respectively, while quiescence is assumed when $\sigma_i = -1$.

The influence of external stimuli, representing e.g. medias in social networks or environmental variations imposing phenotypic changes via gene expression in proteomics or viruses in immune networks, can be encoded by means of a one-body Hamiltonian term $H = \sum_i^V h_i \sigma_i$, with h_i suitable for the particular phenomenon (as brilliantly done by McFadden into the first class of problems [60][45], Eigen in the middle [68] and Burnet in the last class [35][19]). As for collective influences among agents modeling is by far harder.

In the model we are going to develop, each agent $i \in (1, \dots, V)$ is endowed with a set of L characters denoted by a binary string ξ_i of length L . For example, in social context this string may characterize the agent and each entry may have a social meaning (i.e. $\xi_i^{\mu=1}$ may take into account an attitude toward the opposite sex such that if $\xi_i^{\mu=1} = 1$, σ_i likes the opposite sex, otherwise if $\xi_i^{\mu=1} = 0$; in the same way $\xi_i^{\mu=2}$ may accounts for smoking and so on up to L). In gene networks the overlap among bit strings may offer a measure of phylogenetic distance while in immunological context may offer the affinity matrix

built up by strings standing for the antibodies (and anti-antibodies) produced by their corresponding lymphocytes.

Now we want to associate a weighted link among two agents by comparing how many similarities they share (note that $0 - 0$ does not contribute in this scheme, but only $1 - 1$), namely

$$J_{ij} = \sum_{\mu=1}^L \xi_i^\mu \xi_j^\mu. \quad (2.1)$$

This description naturally leads to the emergence of a hierarchical partition of the whole population into a series of layers, each layer being characterized by the sharing of an increasing number of characters. Of course, group membership, apart from defining individual identity, is a primary basis both for social and biological interactions and therefore acquaintanceship. As a result, the interaction strength between individual i and j increases with increasing similarity.

Hence, including both terms (one-body and two-bodies) the model we are describing reads off as

$$H_V(\sigma; \xi) = \frac{1}{V} \sum_{i < j}^V J_{ij}(\xi) \sigma_i \sigma_j + \sum_i^V h_i \sigma_i, \quad (2.2)$$

formally identical to the Hopfield model.

The string characters are randomly distributed according to

$$P(\xi_i^\mu = +1) = \frac{1+a}{2}, \quad P(\xi_i^\mu = 0) = \frac{1-a}{2}, \quad (2.3)$$

in such a way that, by tuning the parameter $a \in [-1, +1]$, the concentration of non null-entries for the i -th string $\rho_i = \sum_\mu \xi_i^\mu$ can be varied. When $a \rightarrow -1$ there is no network and we are left with a non interacting spin system, while when $a \rightarrow +1$ we have that $J_{ij} = L$ for any couple and (renormalization trough L^{-1} apart) we recover the standard Curie-Weiss model.

Further, when $a \neq 0$ the pattern distribution is biased, somehow similarly to the correlations investigated by Amit and coworkers in neural scenarios [13]. Moreover, from Eq.(2.3) we get $\langle \xi_i^\mu \xi_i^\nu \rangle = ((1+a)/2)[\delta_{\mu\nu} + ((1+a)/2)(1 - \delta_{\mu\nu})]$, - apart $a = 0$ which reduces to completely uncorrelated patterns.

As we will see, small values of a give rise to highly correlated, diluted networks, while, as a gets larger the network gets more and more connected and correlation among links vanishes.

Even though the theory is defined at each finite V and L , as standard in statistical mechanics, we are interested in the large V behavior (such that, under central limit theorem permissions, deviations from averaged values become negligible and the theory predictive). To this task we find meaningful to let even L diverge linearly with the system size (to bridge conceptually to high storage neural networks), such that $\lim_{V \rightarrow \infty} L/V = \alpha$ defines α as another control parameter. Finally, since we are interested in the regime of large V and large L we will often confuse V with $V - 1$ and L with $L - 1$.

3 The emergent network

The set of strings $\{\xi_i^\mu\}_{i=1,\dots,V;\mu=1,\dots,L}$ together with the rule in eq. (2.1) generates a weighted graph $\mathcal{G}(V, L, a)$ describing the mutual interactions among nodes. The following investigation is just aimed at the study of its topological features, which, as well known, are intimately connected with the dynamical properties of phenomena occurring on the network itself (e.g. diffusion [26, 2, 5], transport [9, 7], critical properties [31, 8], coherent propagation [6], relaxation [44], just to cite a few). We first focus on the topology neglecting the role of weights and we say that two nodes i and j are connected whenever J_{ij} is strictly positive; disorder on couplings will be addressed in Sec. 3.2

It is immediate to see that the number ρ of non-null (i.e. equal to 1) entries occurring in a string ξ is Bernoulli-distributed, namely

$$P_1(\rho; a, L) = \binom{L}{\rho} \left(\frac{1+a}{2}\right)^\rho \left(\frac{1-a}{2}\right)^{L-\rho}, \quad (3.1)$$

with average and variance, respectively,

$$\bar{\rho}_{a,L} = \sum_{\rho=0}^L \rho P_1(\rho; a, L) = \left(\frac{1+a}{2}\right) L, \quad (3.2)$$

$$\sigma_{a,L}^2 = \overline{\rho^2}_{a,L} - \bar{\rho}_{a,L}^2 = \left(\frac{1-a^2}{4}\right) L. \quad (3.3)$$

Moreover, the probability that a string is made up of null entries only is $\prod_{\mu=1}^L P(\xi_i^\mu = 0) = [(1-a)/2]^L$, thus, since we are allowing repetitions among strings, the number of isolated nodes is at least $V[(1-a)/2]^L$.

Let us consider two strings ξ_i and ξ_j of length L , with ρ_i and ρ_j non-null entries, respectively. Then, the probability $P_{\text{match}}(k; \rho_i, \rho_j, L)$ that such strings display k matching entries is

$$P_{\text{match}}(k; \rho_i, \rho_j, L) = \frac{\binom{L}{k} \binom{L-k}{\rho_i-k} \binom{L-\rho_i}{\rho_j-k}}{\binom{L}{\rho_i} \binom{L}{\rho_j}}, \quad (3.4)$$

which is just the number of arrangements displaying k matchings over the number of all possible arrangements. As anticipated, for two agents to be connected it is sufficient that their coupling (see eq. (2.1)) is larger than zero, i.e. that they share at least one trait. Therefore, we have the following link probability

$$P_{\text{link}}(\rho_i, \rho_j, L) = \sum_{k=1}^L P_{\text{match}}(k; \rho_i, \rho_j, L) = 1 - P_{\text{match}}(0; \rho_i, \rho_j, L) = 1 - \frac{(L-\rho_i)!(L-\rho_j)!}{L!(L-\rho_i-\rho_j)!}. \quad (3.5)$$

The previous expression shows that, in general, the link probability between two nodes does depend on the nodes considered through the related parameters ρ_i and ρ_j : When ρ_i and ρ_j are both large, the nodes are likely to be connected and vice versa. Another kind of correlation, intrinsic to the model, emerges due to the fact that, given $\xi_i^\mu = 1$, the node 1 will be connected with all strings with non-null μ -th entry; this gives rise to a large (local) clustering coefficient c_i (see section 3.4). Such a correlation vanishes

when a is sufficiently larger than -1 , so that any generic couple has a relative large probability to be connected; in this case the resulting topology is well approximated by a highly connected, uncorrelated (Erdős-Renyi) random graph. Moreover, when $a \rightarrow +1$ we recover the fully-connected graph.

Finally, it is important to stress that, according to our assumptions, repetitions among strings are allowed and this, especially for finite L and V , can have dramatic consequences on the topology of the structure. In fact, the suppression of repetitions would spread out the distribution $P_1(\rho; a, L)$, allowing the emergence of strings with a large ρ (with respect to the expected mean value $L(1+a)/2$); such nodes, displaying a large number of connections, would work as hubs. On the other hand, recalling that the number of couples displaying perfect overlapping strings is $\sim V^2/2^L$, we have that in the thermodynamic limit and L growing faster than $\log V$, repetitions among strings have null measure.

3.1 Degree distribution

We focus the attention on an arbitrary string ξ with ρ non-null entries and we calculate the average probability $\bar{P}_{\text{link}}(\rho; a)$ that ξ is connected to another generic string, which reads as

$$\begin{aligned}\bar{P}_{\text{link}}(\rho; a) &= \sum_{\rho_i=0}^L P_1(\rho_i; a, L) P_{\text{link}}(\rho, \rho_i; L) \\ &= 1 - \left(\frac{1-a}{2}\right)^L \left(1 + \frac{1+a}{1-a}\right)^{L-\rho} = 1 - \left(\frac{1-a}{2}\right)^\rho.\end{aligned}\quad (3.6)$$

This result is actually rather intuitive as it states that, in order to be linked to ξ , a generic node has to display at least a non-null entry corresponding to the ρ non-null entries of ξ . Notice that the link probability of eq. (3.6) corresponds to a mean-field approach where we treat all the remaining nodes in the average; accordingly, the degree distribution $P_{\text{degree}}(z; \rho, a, V)$ for ξ gets

$$P_{\text{degree}}(z; \rho, a, V) = \binom{V}{z} \left[1 - \left(\frac{1-a}{2}\right)^\rho\right]^z \left(\frac{1-a}{2}\right)^{\rho(V-z)}.\quad (3.7)$$

Therefore, the number of null-entries controls the degree-distribution of the pertaining node: A large ρ gives rise to narrow (i.e. small variance) distributions peaked at large values of z . Notice that $\bar{P}_{\text{link}}(\rho; a)$ and, accordingly, $P_{\text{degree}}(z; \rho, a, V)$ are independent of L .

More precisely, from eq. (3.7), the average degree for a string displaying ρ non-null entries is

$$\bar{z}_\rho = V \left[1 - \left(\frac{1-a}{2}\right)^\rho\right],\quad (3.8)$$

while the pertaining variance is

$$\sigma_\rho^2 = V \left[1 - \left(\frac{1-a}{2}\right)^\rho\right] \left(\frac{1-a}{2}\right)^\rho.\quad (3.9)$$

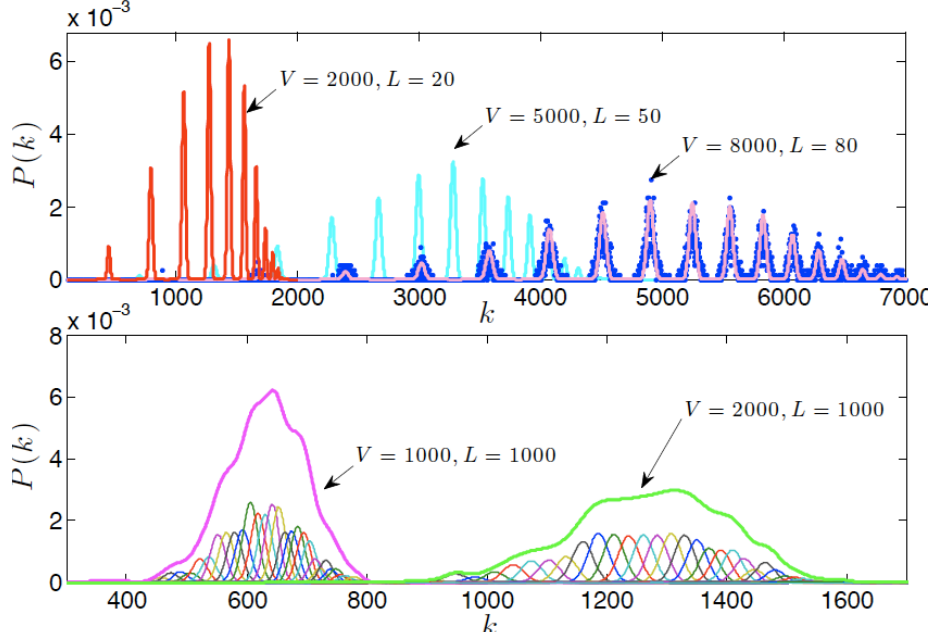


Figure 3.1: Degree distribution $\bar{P}_{\text{degree}}(k)$ for systems displaying small values of L and multimodal distribution (upper panel) and large values of L and distribution collapsing into a unimodal one (lower panel). In the former case we compare systems of different sizes but fixed $\alpha = 0.01$, where continuous lines represent the analytic estimate of eq. (3.10) while symbols (\bullet) represent data from simulations and are reported for clearness only for the case $V = 8000$. In the lower panel we compare systems with same L but different volumes; thicker curves represent $\bar{P}_{\text{degree}}(z; a, L, V)$, while each mode $P_{\text{degree}}(z; \rho, a, V)$ is depicted in different colors.

Now, the overall distribution can be written as a combination of binomial distributions

$$\bar{P}_{\text{degree}}(z; a, L, V) = \sum_{\rho=0}^L P_{\text{degree}}(z; \rho, a, V) P_1(\rho; a, L), \quad (3.10)$$

where the overlap among two “modes”, say ρ and $\rho + 1$, can be estimated through $\sigma_{\rho}/(\bar{z}_{\rho+1} - \bar{z}_{\rho})$: Exploiting eqs. (3.8) and (3.9) we get

$$\frac{\sigma_{\rho}}{\bar{z}_{\rho+1} - \bar{z}_{\rho}} = \sqrt{1 - \left(\frac{1-a}{2}\right)^{\rho}} \left[\sqrt{V} \left(\frac{1-a}{2}\right)^{\rho/2} \left(\frac{1+a}{2}\right) \right]^{-1} \sim \sqrt{\frac{L}{V}} = \sqrt{\alpha}, \quad (3.11)$$

where the generic mode ρ is confused with $\bar{\rho}$ and the approximate result $\sqrt{L/V}$ was derived by using the scaling $a = -1 + \gamma/V^{\theta}$, with $1/2 < \theta \leq 1$ (both these points are fully discussed in the next Section); also, the last passage holds rigorously in the thermodynamic limit of the high storage regime (L linearly

diverging with V). Interestingly, for systems with different scaling regimes among L and V , for instance $L \propto \log V$ [18, 1], the distribution remains multi-modal because a vanishing overlap occurs among the single distributions $P_{\text{degree}}(z; \rho, a, V)$: $\bar{P}_{\text{degree}}(z; a, L, V)$ turns out to be an $(L+1)$ -modal distribution (see Fig. 3.1, upper panel); vice versa, for $L \propto V$, the overall distribution gets mono-modal (see Fig. 3.1, lower panel). Briefly, we mention that for $\theta = 1/2$ the ratio in the l.h.s. of eq. (3.11) still converges to a finite value approaching $\sqrt{\alpha}$ for $\gamma^2 \ll \alpha$, while for $\theta < 1/2$ it diverges.

From eq. (3.10), the average degree for a generic node is

$$\bar{z} = \sum_{z=0}^V z \bar{P}_{\text{degree}}(z; a, L, V) = \sum_{\rho=0}^L P_1(\rho; a, L) \bar{z}_\rho = V \left\{ 1 - \left[1 - \left(\frac{1+a}{2} \right)^2 \right]^L \right\}, \quad (3.12)$$

where

$$p = 1 - \left[1 - \left(\frac{1+a}{2} \right)^2 \right]^L \quad (3.13)$$

is the average link probability for two arbitrary strings ξ_i and ξ_j , which can be obtained by averaging over all possible string arrangements, namely, recalling eqs. (3.1) and (3.6),

$$\begin{aligned} p &= \sum_{\rho_i=0}^L \sum_{\rho_j=0}^L P_1(\rho_i; a, L) P_1(\rho_j; a, L) P_{\text{link}}(\rho_i, \rho_j; a, L) \\ &= 1 - \left(\frac{1-a}{2} \right)^{2L} \sum_{\rho_i=0}^L \sum_{\rho_j=0}^L \left(\frac{1+a}{1-a} \right)^{\rho_i+\rho_j} \binom{L}{\rho_i} \binom{L-\rho_i}{\rho_j} \\ &= 1 - \left[1 - \left(\frac{1+a}{2} \right)^2 \right]^L. \end{aligned} \quad (3.14)$$

Of course, eq. (3.14) could be obtained directly by noticing that the probability for the μ -th entries of two strings not to yield any contribute is $1 - [(1+a)/2]^2$, so that two strings are connected if there is at least one matching.

3.2 Coupling distribution

As explained in Sec. 2, the coupling J_{ij} among nodes i and j is given by the relative number of matching entries among the corresponding strings ξ_i and ξ_j . Eq. (3.4) provides the probability for ξ_i and ξ_j to share a link of magnitude $J = k$, namely $P_{\text{coupling}}(J; \rho_i, \rho_j, L) = P_{\text{match}}(k; \rho_i, \rho_j, L)$. Following the same arguments as in the previous section we get the probability that a link stemming from ξ_i has magnitude J , that is

$$\bar{P}_{\text{coupling}}(J; \rho_i, a) = \sum_{\rho_j=0}^L P_{\text{coupling}}(J; \rho_i, \rho_j, L) P_1(\rho_j; a, L) = \binom{\rho_i}{J} \left(\frac{1-a}{2} \right)^{\rho_i-J} \left(\frac{1+a}{2} \right)^J, \quad (3.15)$$

which is just the probability that J out of ρ_i non-null entries are properly matched with the generic second node.

Similarly to $\bar{P}_{\text{degree}}(z; a, L, V)$, the overall coupling distribution can be written as the superposition $\sum_{\rho} P_1(\rho; a, L) \bar{P}_{\text{coupling}}(J; \rho, a)$, giving rise to a multimodal distribution. Each mode has variance $\sigma_{\rho}^2 = \rho(1 - a^2)/4$ and is peaked at

$$\bar{J}_{\rho} = \rho \frac{1 + a}{2}, \quad (3.16)$$

which represents the average coupling expected for links stemming from a node with ρ non-null entries. Nevertheless, by comparing $\bar{J}_{\rho+1} - \bar{J}_{\rho} = (1 + a)/2$ and the standard deviation $\sqrt{\rho(1 - a^2)}/2$, we find that in the limit $L = \alpha V$ and $V \rightarrow \infty$ the distribution gets mono-modal.

Anyhow, we can still define the average weighted degree w_{ρ} expected for a node displaying ρ non-null entries. Given that for the generic node i , $w \equiv \sum_j J_{ij}$, we get

$$\bar{w}_{\rho} = V \bar{J}_{\rho} = V \rho \frac{1 + a}{2}. \quad (3.17)$$

Of course, one expects that the larger the coordination number of a node and the larger its weighted degree; such a correlation is linear only in the regime of low connectivity. In fact, by merging eq. (3.8) and eq. (3.17), one gets

$$\bar{w}_{\rho} = \left(\frac{1 + a}{2} \right) \frac{\log \left(1 - \frac{\bar{z}_{\rho}}{V} \right)}{\log \left(\frac{1 - a}{2} \right)} V \approx \bar{z}_{\rho}, \quad (3.18)$$

where the last expression holds for $\bar{z}_{\rho} \ll V$ and $a \ll 1$.

It is important to stress that (apart pathological cases which will be taken into account in the $L \rightarrow \infty$ scaling later) the variance of ρ scales as $\sigma_{\rho}^2(a; L) = (1 - a^2)L/4$ such that, despite the average of ρ is $(1 + a)L/2$, substituting ρ/L with $(1 + a)/2$ into eq. (3.18) becomes meaningless in the thermodynamic limit as the variance of \bar{J}_{ρ} diverges as $\sqrt{L} \propto \sqrt{V}$: This will affect drastically the thermodynamics whenever far from the Curie-Weiss limit.

It should be remarked that \bar{J}_{ρ} represents the average coupling for a link stemming from a node characterized by a string with ρ non-null entries, where the average includes also non-existing links corresponding to zero coupling. On the other hand, the ratio $\bar{w}_{\rho}/\bar{z}_{\rho}$ directly provides the average magnitude for existing couplings. Moreover, the average magnitude for a generic link is

$$\bar{J} = \sum_{\rho=0}^L P_1(\rho; a, L) \bar{J}_{\rho} = \left(\frac{1 + a}{2} \right)^2. \quad (3.19)$$

By comparing eq. (3.16) and eq. (3.19) we notice that the local energetic environment seen by a single node, i.e. \bar{J}_{ρ} , and the overall energetic environment, i.e. \bar{J} , scale, respectively, linearly and quadratically with $(1 + a)/2$: we will see in the thermodynamic dedicated section that (apart in the Curie-Weiss limit where global and local effects merge) despite the self-consistence relation (which is more sensible by local condition) will be influenced by $\sqrt{\bar{J}}$, critical behavior will be found at $\beta_c = \bar{J}^{-1}$ coherently with a manifestation of a collective, global effect.

Anyhow, when V is large and the coupling distribution is narrowly peaked at the mode corresponding to $\bar{\rho}_{a,L}$, the couplings can be rather well approximated by the average value $\bar{J}_{L(1+a)/2} = [(1 + a)/2]^2 = \bar{J}$, so that the disorder due to the weight distribution may be lost; as we will show this can occur in the

regime of high dilution ($\theta > 1/2$). As for the other source of disorder (i.e. topological inhomogeneity), this can also be lost if a is sufficiently larger than -1 as we are going to show.

3.3 Scalings in the thermodynamic limit

In the thermodynamic limit and high-storage regime, L is linearly divergent with V and the average probability p for two nodes to be connected (see eq. (3.13)) approaches a discontinuous function assuming value 1 when $a > -1$, and value 0 when $a = -1$. More precisely, as $V \rightarrow \infty$ there exists a vanishingly small range of values for a giving rise to a non-trivial graph; such a range is here recognized by the following scaling

$$a = -1 + \frac{\gamma}{V^\theta}, \quad (3.20)$$

where $\theta \geq 0$ and γ is a finite parameter.

First of all, we notice that, following eqs. (3.2) and (3.3),

$$\bar{\rho}_{-1+\gamma/V^\theta, \alpha V} = \frac{\alpha\gamma}{2V^{\theta-1}} \quad (3.21)$$

$$\sigma_{-1+\gamma/V^\theta, \alpha V}^2 = \frac{\alpha\gamma}{2V^{\theta-1}} \left(1 - \frac{\gamma}{2V^\theta}\right) \sim \bar{\rho}_{-1+\gamma/V^\theta, \alpha V}, \quad (3.22)$$

where the last approximation holds in the thermodynamic limit and it is consistent with the convergence of the binomial distribution in eq. (3.1) to a Poissonian distribution. For $\theta \leq 1$, $\bar{\rho} \gtrsim \sigma$, so that when referring to a generic mode ρ , we can take without loss of generality $\bar{\rho}$; the case $\theta > 1$ will be neglected as it corresponds to a disconnected graph.

Indeed, the probability for two arbitrary nodes to be connected gets

$$p = 1 - \left[1 - \left(\frac{1+a}{2}\right)^2\right]^L = 1 - \left[1 - \frac{\gamma^2}{4V^{2\theta}}\right]^{\alpha V} \xrightarrow{V \rightarrow \infty} 1 - e^{-\gamma^2 \alpha V^{1-2\theta}/4}, \quad (3.23)$$

so that we can distinguish the following regimes:

- $\theta < 1/2$, $p \approx 1$, $\bar{z} \approx V \Rightarrow$ Fully connected (FC) graph
- $\theta = 1/2$, $p \sim 1 - e^{-\gamma^2 \alpha/4} \sim \gamma^2 \alpha/4$, $\bar{z} = O(V) \Rightarrow$ Linearly diverging connectivity
Within a mean-field description the Erdős-Rényi (ER) random graph with finite probability $\mathcal{G}(V, p)$ is recovered.
- $1/2 < \theta < 1$, $p \sim \gamma^2 \alpha V^{1-2\theta}/4$, $\bar{z} = O(V^{2-2\theta}) \Rightarrow$ Extreme dilution regime (ED)
In agreement with [84, 85], $\lim_{V \rightarrow \infty} \bar{z}^{-1} = \lim_{V \rightarrow \infty} \bar{z}/V = 0$.
- $\theta = 1$, $p \sim \frac{\gamma^2 \alpha}{4V}$, $\bar{z} = O(V^0) \Rightarrow$ Finite connectivity regime
Within a mean-field description $\gamma^2 \alpha/4 = 1$ corresponds to a percolation threshold.

Therefore, while θ controls the connectivity regime of the network, γ allows a fine tuning.

As for the average coupling (see eq. (3.19)) and the average weighted degree:

$$\bar{J} = \frac{\gamma^2}{4V^{2\theta}}, \quad (3.24)$$

$$\bar{w} = V\bar{J} = \frac{\gamma^2}{4V^{2\theta-1}}. \quad (3.25)$$

Now, the average “effective coupling” \tilde{J} , obtained by averaging only on existing links, can be estimated as

$$\tilde{J} = \bar{J}/p = \begin{cases} \gamma^2/(4V^{2\theta}) & \text{if } \theta < 1/2 \\ \gamma^2/[4V^{2\theta}(1 - e^{-\gamma^2\alpha/4})] & \text{if } \theta = 1/2 \\ 1/(\alpha V) = 1/L & \text{if } 1/2 < \theta \leq 1 \end{cases} \quad (3.26)$$

Interestingly, this results suggests that in the thermodynamic limit, for values of a determined by eq. (3.20) with $1/2 < \theta \leq 1$, nodes are pairwise either non-connected or connected due to one single matching among the relevant strings. This can be shown more rigorously by recalling the coupling distributions $\bar{P}_{\text{coupling}}(J; \rho_i, L)$ of eq. (3.15): In particular, for $\theta > 1/2$, neglecting higher order corrections, for $J = 0$ the probability is $p_0 \sim \exp(\alpha\gamma^2 V^{1-2\theta}/4) \sim 1 - \gamma^2\alpha/(4V^{2\theta-1})$, for $J = 1/L$ the probability is $p_1 \sim p_0\gamma^2\alpha/(4V^{2\theta-1}) \sim 1 - p_0$. For $\theta = 1/2$ this still holds for $\alpha\gamma^2/4 \ll 1$, which corresponds to a relatively high dilution regime, otherwise some degree of disorder is maintained, being that $p_k \sim (\alpha\gamma^2/4)^k/k!$. On the other hand, for $\theta < 1/2$, while topological disorder is lost (FC), the disorder due to the coupling distribution is still present. However, notice that for $\theta = 0$ and $\gamma = 2$, $\bar{P}_{\text{coupling}}(J; \rho_i, L)$ gets peaked at $J = L$ and, again, disorder on couplings is lost so that a pure Curie-Weiss model is recovered.

This means that, for $L = \alpha V$ and $V \rightarrow \infty$, we can distinguish three main regions in the parameter space (θ, α, γ) where the graph presents only topological disorder ($\theta > 1/2$), or only coupling disorder ($\theta < 1/2$), or both ($\theta = 1/2 \wedge \gamma^2\alpha = O(1)$).

In general, we expect that the critical temperature scales like the connectivity times the average coupling and the system can be looked at as a fully connected with average coupling equal to \bar{J} or as a diluted network with effective coupling \tilde{J} and connectivity given by \bar{z} ; in any case we get $\beta_c^{-1} \sim \bar{J}$ (crf. eq.(4.37)).

3.4 Small-world properties

Small-world networks are endowed, by definition, with high cluster coefficient, i.e. they display sub-networks that are characterized by the presence of connections between almost any two nodes within them, and with small diameter, i.e. the mean-shortest path length among two nodes grows logarithmically (or even slower) with V . While the latter requirement is a common property of random graphs [77, 78], the clustering coefficient deserves much more attention also due to the basic role it covers in biological [86, 87] and social networks [52, 53].

The clustering coefficient measures the likelihood that two neighbors of a node are linked themselves; a higher clustering coefficient indicates a greater “cliquishness”. Two versions of this measure exist [77, 78]:

global and local; as for the latter the coefficient c_i associated to a node i tells how well connected the neighborhood of i is. If the neighborhood is fully connected, c_i is 1, while a value close to 0 means that there are hardly any connections in the neighborhood.

The clustering coefficient of a node is defined as the ratio between the number of connections in the neighborhood of that node and the number of connections if the neighborhood was fully connected. Here neighborhood of node i means the nodes that are connected to i but does not include i itself. Therefore we have

$$c_i = \frac{2E_i}{z_i(z_i - 1)}, \quad (3.27)$$

where E_i is the number of actual links present, while $z_i(z_i - 1)/2$ is the number of connections for a fully connected group of z_i nodes. Of course, for the Erdős-Rényi graph where each link is independently drawn with a probability p , one has $c^{ER} = p$, regardless of the node considered.

We now estimate the clustering coefficient for the graph $\mathcal{G}(a, L, V)$, focusing the attention on a range of a such that the average number of non-null entries per string is small enough for the link probability to be strictly lower than 1 so that the topology is non trivial; to fix ideas and recalling last section $1/2 \leq \theta \leq 1$. Let us consider a string displaying ρ non-null entries, corresponding to the positions $\mu_1, \mu_2, \dots, \mu_\rho$, and z nearest-neighbors; the latter can be divided in ρ groups: strings belonging to the j -th group have $\xi^{\mu_j} = 1$. Neglecting the possibility that a nearest-neighbor can belong to more than one group contemporary (in the thermodynamic limit this is consistent with Eq. 3.26), we denote with n_j the number of nodes belonging to the j -th group, being $\sum_j n_j = z$, whose average value is z/ρ (which, due to the above assumptions is larger than one). Now, nodes belonging to the same group are all connected with each other as they share at least one common trait, i.e. they form a clique; the contribute of intra-group links is

$$E_{\text{intra}} = \frac{1}{2} \sum_{i=1}^{\rho} n_i(n_i - 1) = \frac{1}{2} \left(\sum_{i=1}^{\rho} n_i^2 - z \right) \approx \frac{1}{2} \left[\left(\frac{z}{\rho} \right)^2 \rho - z \right], \quad (3.28)$$

while the contribute of inter-group links can be estimated as

$$E_{\text{inter}} \approx \sum_{i,j=1, i \neq j}^{\rho} n_i n_j \tilde{p} \approx \left(\frac{z}{\rho} \right)^2 \binom{\rho}{2} \tilde{p}, \quad (3.29)$$

where \tilde{p} is the probability for two nodes linked to i and belonging to different groups to be connected, and the sum runs over all possible $\binom{\rho}{2}$ couples of groups. Hence, the total number of links among neighbors is $E = E_{\text{intra}} + E_{\text{inter}} = \{ \sum_{i=1}^{\rho} n_i \sum_{j=1}^{\rho} n_j [\tilde{p} + (1 - \tilde{p})\delta_{ij}] - z \} / 2$, where δ_{ij} is the Kronecker delta returning 1 if $i = j$ and zero otherwise; of course, for $\tilde{p} = 1$ we have $E = (z^2 - z)/2$ and $c_i = 1$.

Now, in the average, the probability \tilde{p} is smaller than p as it represents the probability for two strings of length $L - 1$ and displaying an average number of non-null entries equal to $\rho - 1$ to be connected. However, for ρ and L not too small the two probabilities converge so that by summing the two contributes in eq. (3.28) and (3.29) we get

$$E \approx \frac{1}{2} \left[\left(\frac{z}{\rho} \right)^2 \rho - z \right] + \left(\frac{z}{\rho} \right)^2 \binom{\rho}{2} \tilde{p} \Rightarrow c \approx p + \frac{1}{\rho} - \frac{1}{z - 1} > p, \quad (3.30)$$

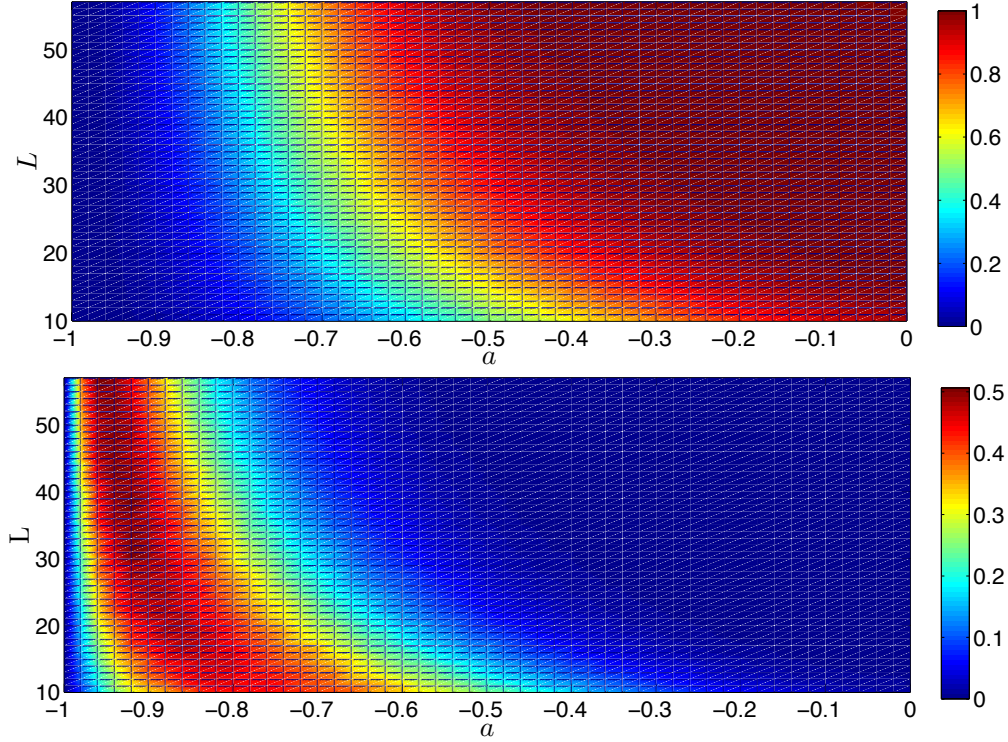


Figure 3.2: Upper panel: average link probability $p = \bar{z}/N$; Lower panel: difference between the average clustering coefficient for $\mathcal{G}(V, L, a)$ and for an analogous ER graph just corresponding to p . Both plots are presented as function of a and L and refer to a system of $V = 2000$ nodes.

where in the last inequality we used $\rho < z - 1$. Therefore, it follows straightforward that c_i is larger than the clustering coefficient expected for an ER graph displaying the same connectivity, that is $c^{ER} = p$.

From previous arguments it is clear that the SW effect gets more evident, with respect to the ER case taken as reference, when the network is highly diluted. This is confirmed by numerical data: Fig. 3.2 shows in the lower panel the clustering coefficient expected for the analogous ER graph, namely $c^{ER} = \bar{z}/V$, while in the upper panel it shows the difference between the average local clustering coefficient $c = \sum_{i=1}^V c_i/V$ and c^{ER} itself. Of course, when a approaches 1, the graph gets fully connected and $c \rightarrow c^{ER} \rightarrow 1$.

Finally we mention that when focusing on the low storage regime, a non-trivial distribution for couplings can give rise to interesting effects. Indeed, weak ties can be shown [88] to work as bridges connecting communities strongly linked up, as typical of real networks [52, 89]. Also, as often found in technological and biological networks, the graph under study display a “dissortative mixing” [77, 78], that is to say, high-degree vertices prefer to attach to low-degree nodes [88].

4 Thermodynamics

So far the emergent network has been exhaustively described by a random, correlated graph whose links are endowed with weights; we now build up a quantitative thermodynamics on such a structure.

Once the Hamiltonian $H_V(\sigma; \xi)$ is given (eq. 2.2), we can introduce the partition function $Z_V(\beta; \xi)$ as

$$Z_V(\beta; \xi) = \sum_{\sigma} e^{-\beta H_V(\sigma; \xi)}, \quad (4.1)$$

the Boltzmann state ω as

$$\omega(\cdot) = \frac{\sum_{\sigma} \cdot e^{-\beta H_V(\sigma; \xi)}}{Z_V(\beta; \xi)}, \quad (4.2)$$

and the related free energy as

$$A(\beta, \alpha, a) = \lim_{V \rightarrow \infty} \frac{1}{V} \mathbb{E} \log Z_V(\beta; \xi), \quad (4.3)$$

where \mathbb{E} averages over the quenched distributions of the affinities ξ .

Once the free energy (or equivalently the *pressure*) is obtained, remembering that (calling S the entropy and U the internal energy)

$$A(\beta, \alpha, a) = -\beta f(\beta, \alpha, a) = S(\beta, \alpha, a) - \beta U(\beta, \alpha, a),$$

the whole macroscopic properties, thermodynamics, can be derived due the Legendre structure of thermodynamic potentials [67].

4.1 Free energy trough extended double stochastic stability

For the sake of clearness now we expose in complete generality and details the whole plan dealing with a generic expectation on ξ (i.e. $\mathbb{E}\xi = (1+a)/2$), then, we will study the $L \rightarrow \infty$ scaling, in which a must tend to -1 more carefully.

With this palimpsest in mind, let us normalize the Hamiltonian (2.2) in a more convenient form for this section (i.e. dividing by L the J_{ij} , such that the effective coupling is bounded by 1), and let us neglect the external field h which can be implemented later straightforwardly.

$$H_V(\sigma; \xi) = \frac{1}{VL} \sum_{ij}^V \sum_{\mu}^L \xi_i^{\mu} \xi_j^{\mu} \sigma_i \sigma_j. \quad (4.4)$$

As a next step, through the Hubbard-Stratonovick transformation [67, 41], we map the partition function of our Hamiltonian into a bipartite Erdős-Rényi ferromagnetic random graph [3][47], whose parties are the former built by the V agents and a new one built of by L Gaussian variables z_{μ} , $\mu \in (1, \dots, L)$:

$$Z(\beta; \xi) = \sum_{\sigma} \exp(-\beta H_V(\sigma; \xi)) = \sum_{\sigma} \int_{-\infty}^{+\infty} \prod_{\mu=1}^L d\mu(z_{\mu}) \exp\left(\sqrt{\frac{\beta}{LV}} \sum_i^V \sum_{\mu}^L \xi_{i,\mu} \sigma_i z_{\mu}\right), \quad (4.5)$$

where with $\prod_{\mu=1}^L d\mu(z_\mu)$ we mean the Gaussian measure on the product space of the Gaussian party. Note that, even when L goes to infinity linearly with V (as in the high storage Hopfield model [11]), due to the normalization encoded into the affinity product of the ξ 's nor the z -diagonal term contribute to the free energy (as happens in the neural network counterpart [23]), neither (but this will be clear at the end of the section) there is a true dependence by α in the thermodynamics.

Furthermore, notice that the graph of the interactions among the two parties is now a simple, and no longer weighted, Erdős-Rényi [14]: so we started with a complex topology for a single party and we turned this problem in solving the thermodynamics for a simpler topology but paying the price of accounting for another party in interaction. The lack of weight on links will have fundamental importance when defining the order parameters.

Another approach to this is noticing that if we dilute -randomly- directly the Hopfield model (i.e. as checking for its robustness as already tested by Amit [10]) we push it on an Erdos-Renyi topology, while if we dilute its entries in pattern definitions (due to the Hebbian kernel) we have to deal with correlated dilution.

Consequently (strictly speaking assuming the existence of the V limit) we want to solve for the following free energy:

$$A(\beta, \alpha, a) = \lim_{V \rightarrow \infty} \frac{1}{V} \mathbb{E} \log \sum_{\sigma} \int_{-\infty}^{+\infty} \prod_{\mu}^L d\mu(z_{\mu}) \exp \left(\sqrt{\frac{\beta}{LV}} \sum_i^V \sum_{\mu}^L \xi_{i,\mu} \sigma_i z_{\mu} \right). \quad (4.6)$$

To this task we extend the method of the double stochastic stability recently developed in [23] in the context of neural networks. Namely we introduce independent random fields $\eta_i, i \in (1, \dots, V)$ and $\chi_{\mu}, \mu \in (1, \dots, L)$, (whose probability distribution is the same as for the ξ variables -as in every cavity approach-), which account for one-body interactions for the agents of the two parties. So our task is to interpolate among the original system and the one left with only these random perturbations: Let us use $t \in [0, 1]$ for such an interpolation; the trial free energy $A(t)$ is then introduced as follows

$$\begin{aligned} A(t) &= \lim_{V \rightarrow \infty} \frac{1}{V} \mathbb{E} \log \sum_{\sigma} \int_{-\infty}^{+\infty} \prod_{\mu}^L d\mu(z_{\mu}) \cdot \\ &\cdot \exp \left(t \sqrt{\frac{\beta}{LV}} \sum_{i\mu}^{VL} \xi_{i\mu} \sigma_i z_{\mu} + (1-t) \left[\sum_{l_c=1}^L b_{l_c} \sum_i^V \eta_i \sigma_i + \sum_{l_b=1}^V c_{l_b} \sum_{\mu}^L \chi_{\mu} z_{\mu} \right] \right), \end{aligned} \quad (4.7)$$

where now $\mathbb{E} = \mathbb{E}_{\xi} \mathbb{E}_{\eta} \mathbb{E}_{\chi}$ and b_{l_c} [with $l_c \in (1, \dots, L)$], and c_{l_b} [with $l_b \in (1, \dots, V)$] are real numbers (possibly functions of β, α) to be set a posteriori.

As the theory is no longer Gaussian, we need infinite sets of random fields (mapping the presence of multi-overlaps in standard dilution[3][43] and no longer only the first two momenta of the distributions). Of course we recover the proper free energy by evaluating the trial $A(t)$ at $t = 1$, ($A(\beta, \alpha, a) = A(t = 1)$), which we want to obtain by using the fundamental theorem of calculus:

$$A(1) = A(0) + \int_0^1 \left(\partial A(t') / \partial t' \right)_{t'=t} dt. \quad (4.8)$$

To this task we need two objects: The trial free energy $A(t)$ evaluated at $t = 0$ and its t -streaming $\partial_t A(t)$.

Before outlining the calculations, some definitions are in order here to lighten the notation: taken g as

a generic function of the quenched variables we have

$$\mathbb{E}_\eta g(\eta) = \sum_{l_b=0}^V P(l_b) g(\eta_{l_b}) = \sum_{l_b=0}^V \binom{V}{l_b} \left(\frac{1+a}{2}\right)^{V-l_b} \left(\frac{1-a}{2}\right)^{l_b} g(\eta_{l_b}), \quad (4.9)$$

$$\mathbb{E}_\chi g(\chi) = \sum_{l_c=0}^L P(l_c) g(\chi_{l_c}) = \sum_{l_c=0}^L \binom{L}{l_c} \left(\frac{1+a}{2}\right)^{L-l_c} \left(\frac{1-a}{2}\right)^{l_c} g(\chi_{l_c}), \quad (4.10)$$

$$\mathbb{E}_\xi g(\xi) = \sum_{l_b=0}^V \sum_{l_c=0}^L \binom{V}{l_b} \binom{L}{l_c} \left(\frac{1+a}{2}\right)^{l_b+l_c} \left(\frac{1-a}{2}\right)^{V+L-l_b-l_c} \delta_{l_b l_c = l}, \quad (4.11)$$

where $P(l_b)$ is the probability that l_b (out of V random fields) are active, i.e. $\eta = 1$, so that the number of spins effectively contributing to the function g is l_b ; analogously, mutatis mutandis, for $P(l_c)$. Moreover, in the last equation we summed over the probability $P(l)$ that in the bipartite graph a number l of links out of the possible $V \times L$ display a non-null coupling, i.e. $\xi \neq 0$; interestingly, eq. (4.10) can be rewritten in terms of the above mentioned $P(l_b)$ and $P(l_c)$. In fact, $\xi_{i,\mu}$ can be looked at as an $V \times L$ matrix generated by the product of two given vectors like η and χ , namely $\xi_{i,\mu} = \eta_i \chi_\mu$, in such a way that the number of non-null entries in the overall matrix ξ is just given by the number of non-null entries displayed by η times the number of non-null entries displayed by χ . Hence, $P(l)$ is the product of $P(l_b)$ and $P(l_c)$ conditional to $l_b l_c = l$.

4.2 The ‘topologically microcanonical’ order parameters

Starting with the streaming of eq. (4.7), this operation gives raise to the sum of three terms $\mathcal{A} + \mathcal{B} + \mathcal{C}$. The former when deriving the first contribution into the exponential, the last two terms when deriving the two contributions by all the η and χ .

$$\mathcal{A} = +\frac{1}{V} \sqrt{\frac{\beta}{LV}} \sum_{i,\mu}^{V,L} \mathbb{E} \xi_{i\mu} \omega(\sigma_i z_\mu) = \sqrt{\alpha\beta} \left(\frac{1+a}{2}\right) \sum_{l_b, l_c}^{V,L} P(l_b) P(l_c) M_{l_b} N_{l_c} \quad (4.12)$$

$$\mathcal{B} = -\sum_{l_c=1}^L \frac{b_{l_c}}{V} \sum_i^V \mathbb{E} \eta_i \omega(\sigma_i) = -\sum_{l_c=1}^L b_{l_c} \left(\frac{1+a}{2}\right) \sum_{l_b=0}^V P(l_b) M_{l_b} \quad (4.13)$$

$$\mathcal{C} = -\sum_{l_b=1}^V \frac{c_{l_b}}{N} \sum_\mu^L \mathbb{E} \chi_\mu \omega(z_\mu) = -\sqrt{\alpha} \sum_{l_b=1}^V c_{l_b} \left(\frac{1+a}{2}\right) \sum_{l_c=0}^L P(l_c) N_{l_c}, \quad (4.14)$$

where we introduced the following order parameters

$$M_{l_b} = \frac{1}{V} \sum_i^V \omega_{l_b+1}(\sigma_i), \quad (4.15)$$

$$N_{l_c} = \frac{1}{L} \sum_\mu^L \omega_{l_c+1}(z_\mu), \quad (4.16)$$

and the Boltzmann states ω_k are defined by taking into account only k terms among the elements of the party involved.

Of course the Boltzmann states are no longer the ones introduced into the definition (4.2) but the extended ones taking into account the interpolating structure of the cavity fields (which however will recover the originals of statistical mechanics when evaluated at $t = 1$).

Namely, ω_{l_b+1} has only $l_b + 1$ terms of the type $b\sigma$ in the Maxwell-Boltzmann exponential, ultimately accounting for the (all equivalent in distribution) $l_b + 1$ values of $\eta = 1$, all the others being zero.

In the same way ω_{l_c+1} has only $l_c + 1$ terms of the type cz in the Maxwell-Boltzmann exponential, ultimately accounting for the (all equivalent in distribution) $l_c + 1$ values of $\chi = 1$, all the others being zero.

When dealing with $\xi_{i\mu}$ we can decompose the latter accordingly to what discussed before. By these “partial Boltzmann states” we can define the averages of the order parameters as

$$\langle M \rangle = \sum_{l_b}^{V-1} P(l_b) M_{l_b}, \quad (4.17)$$

$$\langle N \rangle = \sum_{l_c}^{L-1} P(l_c) N_{l_c}. \quad (4.18)$$

These objects may deserve more explanations because, as a main difference with classical approaches [3][39][43], here replicas and their overlaps are not involved (somehow suggesting the implicit correctness of a replica symmetric scenario). Conversely, we do conceptually two (standard) operations when introducing our order parameters: at first we average over the (t -extended) Boltzmann measure, then we average over the quenched distributions. Let us consider only one party for simplicity: during the first operation we do not take the whole party size but only a subsystem, say k spins (whose distribution is symmetric with respect to 0 for both the parties, $-1, +1$ for the dichotomic, Gaussians for the continuous one). Then, in the second average, for any k from 1 to the volume of the party, we consider all the possible links among these k nodes in this subgraph. As the links connecting the nodes are always constant (i.e. equal to one due to the Hubbard-Stratonovich transformation (4.4)) in the intensity, the resulting associated energies are, in distribution and in the thermodynamic limit, all equivalent: We are introducing a family of microcanonical observables which sum up to a canonical one, in some sense close to the decomposition introduced in [22].

4.3 The sum rule

Let us now move on and consider the following source S of the fluctuations of the order parameters, where $\bar{M}_{l_b}, \bar{N}_{l_c}$ stand for the replica symmetric values⁴ of the previously introduced order parameters:

$$S = \left(\frac{1+a}{2} \right) \sqrt{\alpha\beta} \sum_{l_b}^{V-1} \sum_{l_c}^{L-1} P(l_b) P(l_c) \left((M_{l_b} - \bar{M}_{l_b})(N_{l_c} - \bar{N}_{l_c}) \right) \quad (4.19)$$

$$= \left(\frac{1+a}{2} \right) \sqrt{\alpha\beta} \langle (M - \bar{M})(N - \bar{N}) \rangle. \quad (4.20)$$

⁴strictly speaking there are no replicas here but configurations over different graphs. However the expression RS-approximation, meaning that we assume the probability distribution of the order parameters delta-like over their average (denoted with a bar) is a sort of self-averaging and is an hinge in disordered statistical mechanics such that we allow ourselves to retain the same expression with a little abuse of language.

We see that with the choice of the parameters $b_{l_c} = \sqrt{\alpha\beta}\bar{N}_{l_c}$ and $c_{l_b} = \sqrt{\beta/\alpha}\bar{M}_{l_b}$, we can write the t -streaming as

$$\dot{A} = S - \frac{1+a}{2}\sqrt{\alpha\beta} \sum_{l_b}^{V-1} \sum_{l_c}^{L-1} P(l_b)P(l_c)\bar{M}_{l_b}\bar{N}_{l_c}.$$

The replica symmetric solution (which is claimed to be the correct expression in diluted ferromagnets) is simply achieved by setting $S = 0$ and forgetting it from future calculations.

We must now evaluate $A(0)$. This term is given by two separate contributions, each for each party. Namely we have

$$\begin{aligned} A(0) &= \frac{1}{V}\mathbb{E} \log \sum_{\sigma} e^{\sum_{l_c=1}^L b_{l_c} \sum_i^V \eta_i \sigma_i} + \frac{1}{V}\mathbb{E} \log \int_{-\infty}^{+\infty} \prod_{\mu=0}^L d\mu(z_{\mu}) e^{\sum_{l_b=1}^V c_{l_b} \sum_{\mu}^L \chi_{\mu} z_{\mu}} \\ &= \log 2 + \left(\frac{1+a}{2}\right) \sum_{l_b=0}^{V-1} P(l_b) \sum_{l_c=0}^{L-1} P(l_c) \log \cosh \left(\sqrt{\alpha\beta}\bar{N}_{l_c}\right) + \left(\frac{1+a}{2}\right)^2 \frac{\beta}{2} \sum_{l_b}^{V-1} P(l_b)\bar{M}_{l_b}^2. \end{aligned}$$

Summing $A(0)$ plus the integral of $\partial_t[A(S=0)]$ we finally get

$$A(t=1) = \log 2 + \left(\frac{1+a}{2}\right) \sum_{l_c}^{L-1} \sum_{l_b}^{V-1} P(l_c)P(l_b) \log \cosh \left(\sqrt{\alpha\beta}\bar{N}_{l_c}\right) \quad (4.21)$$

$$+ \frac{\beta}{2} \left(\frac{1+a}{2}\right)^2 \sum_{l_b}^{L-1} P(l_b)\bar{M}_{l_b}^2 - \frac{1+a}{2}\sqrt{\alpha\beta} \sum_{l_b}^{V-1} \sum_{l_c}^{L-1} P(l_b)P(l_c)\bar{M}_{l_b}\bar{N}_{l_c}. \quad (4.22)$$

It is possible to show that (as each bipartite ferromagnetic model [23][48]) the free energy obeys a min-max principle by which, extremizing the free energy with respect to the order parameters we can express $\langle\bar{N}\rangle$ trough $\langle\bar{M}\rangle$: The trial replica symmetric solution, expressed trough $\langle\bar{M}\rangle, \langle\bar{N}\rangle$ is (at fixed $\langle\bar{N}\rangle$) convex in $\langle\bar{M}\rangle$. This defines uniquely a value $\langle\bar{M}(\bar{N})\rangle$ where we get the max. Further, $\langle\bar{M}(\bar{N})\rangle$ is increasing and convex in $\langle\bar{N}^2\rangle$ such that the following extremization is a well defined procedure.

$$\sum_k P(k) \frac{\partial A}{\partial \bar{M}_k} = 0 \rightarrow \sum_{l_c} P(l_c)\bar{N}_{l_c} = \sum_k P(k) \frac{1+a}{2} \sqrt{\frac{\beta}{\alpha}} \bar{M}_k, \quad (4.23)$$

$$\sum_k P(k) \frac{\partial A}{\partial \bar{N}_{l_k}} = 0 \rightarrow \sum_{l_b} P(l_b)\bar{M}_{l_b} = \sum_k P(k) \tanh \left(\sqrt{\alpha\beta}\bar{N}_k\right). \quad (4.24)$$

Due to the mean field nature of the model, as we can express \bar{N}_k trough the average of the \bar{M}_k , we can write the free energy of our network trough the series of \bar{M}_{l_b} alone [as expected as we started by eq. (2.2)]

$$\begin{aligned} A(\beta, a) &= \log 2 + \left(\frac{1+a}{2}\right) \log \cosh \left(\tanh^{-1} \left[\sum_{l_b} P(l_b)\bar{M}_{l_b} \right] \right) \\ &+ \frac{\beta}{2} \left(\frac{1+a}{2}\right)^2 \sum_{l_b} P(l_b)\bar{M}_{l_b}^2 - \left(\frac{1+a}{2}\right) \sum_{l_b} P(l_b)\bar{M}_{l_b} \tanh^{-1} \left(\sum_{l'_b} P(l_{b'})\bar{M}_{l'_b} \right). \end{aligned} \quad (4.25)$$

As anticipated there is no true dependence by α . Note that without normalizing the scalar product among the bit strings we should rescale β accordingly with α , as in the $L \rightarrow \infty$ limit we would get an

infinite coupling (which is physically meaningless).

Before exploring further properties of these networks, we should recover the well known limit of Curie-Weiss $a = +1$ and isolate spin system $a = -1$.

Let us work out for the sake of clearness the self-consistency in a purely Curie-Weiss style by extremizing, with respect to $\langle \bar{M} \rangle$ eq. (4.25):

$$\begin{aligned} \partial_{\langle \bar{M} \rangle} A(\beta) &= \left(\frac{1+a}{2} \right) \left(\frac{\langle \bar{M} \rangle}{1 - \langle \bar{M} \rangle^2} + \beta \left(\frac{1+a}{2} \right) \langle \bar{M} \rangle \right) - \left(\frac{1+a}{2} \right) \left(\frac{\langle \bar{M} \rangle}{1 - \langle \bar{M} \rangle^2} + \tanh^{-1} \langle \bar{M} \rangle \right) = 0 \\ \Rightarrow \langle \bar{M} \rangle &= \tanh \left(\beta \left(\frac{1+a}{2} \right) \langle \bar{M} \rangle \right) \Rightarrow \tanh^{-1} \langle \bar{M} \rangle = \beta \left(\frac{1+a}{2} \right) \langle \bar{M} \rangle, \end{aligned} \quad (4.26)$$

such that to get the classical magnetization in our model we have to sum overall the contributing graphs, namely $\langle M_{CW} \rangle = \langle \bar{M} \rangle = \sum_{l_b} P(l_b) \bar{M}_{l_b}$, and we immediately recover

$$a \rightarrow -1 \Rightarrow A(\beta, a = -1) = \log 2, \quad (4.27)$$

$$a = +1 \Rightarrow A(\beta, a = +1) = \log 2 + \log \cosh(\beta \langle \bar{M} \rangle) - \frac{\beta}{2} \langle M^2 \rangle, \quad (4.28)$$

which are the correct limits (note that in eq. (4.27) $J = 0$, while in eq. (4.28) $J = 1$).

Furthermore, we stress that in our “topological microcanonical” decomposition of our order parameters, when summing over all the possible subgraphs to obtain the CW magnetization, these are all null apart the only surviving of the fully connected network, so the distribution of the order parameters becomes trivially $\propto \delta(M - M_{CW})$, namely, only one order parameter survives, the classical Curie-Weiss magnetization.

4.4 Critical line trough fluctuation theory

Developing a fluctuation theory of the order parameters allows to determine where critical behavior arises and, ultimately, the existence of a phase transition⁵.

To this task we have at first to work out the general streaming equation with respect to the t -flux. Given a generic observable \mathcal{O} defined on the space of the σ, z variables, it is immediate to check that the following relation holds (we set $\alpha = 1$ for the sake of simplicity as it never appears in the calculations (as can be easily checked by substituting $\langle N \rangle$ with $\langle M \rangle$ trough eq. (4.23) which changes the prefactor from $(\frac{1+a}{2})\sqrt{\alpha\beta} \rightarrow (\frac{1+a}{2})^2\beta$ and express the fluctuations only via the real variables σ ⁶):

$$\frac{\partial \langle \mathcal{O} \rangle}{\partial t} = \frac{1+a}{2} \sqrt{\beta} \left[(\langle \mathcal{O} \mathcal{M} \mathcal{N} \rangle - \langle \mathcal{O} \rangle \langle \mathcal{M} \mathcal{N} \rangle) - \bar{N} (\langle \mathcal{O} \mathcal{M} \rangle - \langle \mathcal{O} \rangle \langle \mathcal{M} \rangle) - \bar{M} (\langle \mathcal{O} \mathcal{N} \rangle - \langle \mathcal{O} \rangle \langle \mathcal{N} \rangle) \right], \quad (4.29)$$

where we defined the centered and rescaled order parameters:

$$\langle \mathcal{M} \rangle = \sqrt{V} \sum_{l_b} P(l_b) (M_{l_b} - \bar{M}_{l_b}) = \sqrt{V} \langle M - \bar{M} \rangle, \quad (4.30)$$

$$\langle \mathcal{N} \rangle = \sqrt{L} \sum_{l_c} P(l_c) (N - \bar{N}) = \sqrt{L} \langle N - \bar{N} \rangle. \quad (4.31)$$

⁵Strictly speaking this approach holds only for second order phase transition, which indeed is the one expected in imitative models, even in presence of dilution [3].

⁶Another simple argument to understand the useless of α is a comparison among neural networks: in that context, α rules -in the thermodynamic limit- the velocity by which we add stored memories into the network with respect to the velocity by which we add neurons. If the former are faster than a critical value, by a TLC argument they sum up to a Gaussian before the infinite volume limit has been achieved and the Hopfield model turns into an SK[23]. Here there is no danger in this as we have only positive -normalized- interactions.

Now we focus on their squares: We want to obtain the behavior of $\langle \mathcal{M}^2 \rangle_{t=1}$, $\langle \mathcal{M}\mathcal{N} \rangle_{t=1}$, $\langle \mathcal{N}^2 \rangle_{t=1}$, so to see where their divergencies (onsetting the phase transition) are located.

By defining the dot operator as

$$\langle \dot{\mathcal{O}} \rangle = \left(\frac{1+a}{2} \right) \sqrt{\beta} \partial_t \langle \mathcal{O} \rangle \quad (4.32)$$

we can write

$$\begin{aligned} \langle \dot{\mathcal{M}}^2 \rangle &= \left[\langle \mathcal{M}^3 \mathcal{N} \rangle - \langle \mathcal{M}^2 \rangle \langle \mathcal{M} \mathcal{N} \rangle - \bar{N} \langle \mathcal{M}^3 \rangle + \bar{N} \langle \mathcal{M}^2 \rangle \langle \mathcal{M} \rangle - \bar{M} \langle \mathcal{M}^2 \mathcal{N} \rangle + \bar{M} \langle \mathcal{M}^2 \mathcal{N} \rangle \right], \\ \langle \dot{\mathcal{M}} \mathcal{N} \rangle &= \left[\langle \mathcal{M}^2 \mathcal{N}^2 \rangle - \langle \mathcal{M} \mathcal{N} \rangle \langle \mathcal{M} \mathcal{N} \rangle - \bar{N} (\langle \mathcal{M}^2 \mathcal{N} \rangle - \langle \mathcal{M} \mathcal{N} \rangle \langle \mathcal{M} \rangle) - \bar{M} (\langle \mathcal{M} \mathcal{N}^2 \rangle - \langle \mathcal{M} \mathcal{N} \rangle \langle \mathcal{N} \rangle) \right], \\ \langle \dot{\mathcal{N}}^2 \rangle &= \left[\langle \mathcal{N}^3 \mathcal{M} \rangle - \langle \mathcal{N}^2 \rangle \langle \mathcal{M} \mathcal{N} \rangle - \bar{N} \langle \mathcal{N}^2 \mathcal{M} \rangle + \bar{N} \langle \mathcal{N}^2 \rangle \langle \mathcal{M} \rangle - \bar{M} \langle \mathcal{N}^3 \rangle + \bar{M} \langle \mathcal{N}^2 \rangle \langle \mathcal{N} \rangle \right]. \end{aligned}$$

Now, for the sake of simplicity, let us introduce alternative labels for the fundamental observables. We define $A(t) = \langle \mathcal{M}^2 \rangle_t$, $D(t) = \langle \mathcal{M} \mathcal{N} \rangle_t$ and $G(t) = \langle \mathcal{N}^2 \rangle_t$ and let us work out their $t = 0$ value, which is straightforward as at $t = 0$ everything is factorized (alternatively these can be seen as high noise expectations):

$$A(t=0) = 1, \quad D(t=0) = 0, \quad G(t=0) = \left(1 + \left(\frac{1+a}{2} \right)^2 \frac{\beta}{\alpha} \langle \bar{M}^2 \rangle \right) - \langle \bar{N}^2 \rangle = 1$$

where we used the self-consistence relation (4.23) and assumed that at least where everything is completely factorized the replica solution is the true solution⁷. Following the technique introduced in [51], starting from the high temperature and, under the Gaussian ansatz for critical fluctuations, we want to take into account correlations among the order parameters. Within this approach, using Wick theorem to split the four observable averages in series of couples, the (formal) dynamical system reduces to

$$\dot{A}(t) = 2A(t)D(t), \quad (4.33)$$

$$\dot{D}(t) = A(t)G(t) + D^2(t), \quad (4.34)$$

$$\dot{G}(t) = 2G(t)D(t). \quad (4.35)$$

We must now solve for $A(t)$, $D(t)$, $G(t)$ and evaluate these expression at $t = \frac{1+a}{2} \sqrt{\beta}$ accordingly to the definition of the dot operator in eq.(4.32). Notice at first that

$$\partial_t \log A = \frac{\dot{A}}{A} = 2D = \frac{\dot{G}}{G} = \partial_t \log G.$$

This means $\partial_t(A/G) = 0$ and as $A(0)/G(0) = 1$ we already know that $A(t) = G(t)$: the fluctuations of the two order parameters behave in the same way, not surprisingly, as already pointed out their mutual interdependence several times.

We are left with

$$\dot{D}(t) = G^2(t) + D^2(t), \quad (4.36)$$

$$\dot{G}(t) = 2G(t)D(t). \quad (4.37)$$

By defining $Y = D + G$ we immediately get, summing the two equations above: $\dot{Y} = Y^2$ by which we get $Y(t) = Y(0)/(1 - tY(0))$. As $Y(0) = 1$ we obtain that

$$D(t = (\frac{1+a}{2})\sqrt{\beta}) + G(t = (\frac{1+a}{2})\sqrt{\beta}) = \frac{1}{1 - (\frac{1+a}{2})\sqrt{\beta}},$$

⁷Any debate concerning RSB on diluted ferromagnets is however ruled out here as we are approaching the critical line from above.

so there is a regular behavior up to $\beta_c = 1/(\frac{1+a}{2})^2$.

We must now solve separately for D and G : this is straightforward by introducing the function $Z = G^{-1}$ and checking that Z obeys

$$-\dot{Z} - 2YZ + 2 = 0,$$

which, once solved with standard techniques (as Y is known) gives $G(t) = [2(1-t)]^{-1}$ and ultimately, simply by noticing the divergencies of $A(t = (1+a)\sqrt{\beta}/2)$, $D(t = (1+a)\sqrt{\beta}/2)$, $G(t = (1+a)\sqrt{\beta}/2)$, we get the critical line for both the squared order parameters and their relative correlation: All these functions do diverge on the line

$$\beta_c = \frac{1}{(\frac{1+a}{2})^2} = \frac{1}{J}, \quad (4.38)$$

defining a phase transition according with intuition.

4.5 $L \rightarrow \infty$ scaling in the thermodynamic limit

As we understood in Section (3.3), in the $V \rightarrow \infty$ and $L \rightarrow \infty$ limits we need to tune the limit of $a \rightarrow -1$ carefully to recover the various interesting topologies and to avoid the trivial limits of fully connected/disconnected graph.

In particular, a must approach -1 as $a = -1 + \gamma/V^\theta$. To tackle this scaling it is convenient to use directly γ, θ as tunable parameter and rewrite the Hamiltonian in the following forms⁸

$$H_V(\sigma; \xi) = \frac{1}{2\alpha V^{2(1-\theta)}} \sum_{ij}^V \sum_{\mu}^L \xi_i^\mu \xi_j^\mu \sigma_i \sigma_j \Rightarrow \tilde{H}_{V,L}(\sigma, z; \xi) = \frac{\sqrt{\beta/\alpha}}{V^{1-\theta}} \sum_{i,\mu} \xi_{i,\mu} \sigma_i z_\mu, \quad (4.39)$$

where the difference among the two expression H, \tilde{H} is due to the Hubbard-Stratonovick transformation applied to the coupled partition functions, as performed early through eq.(4.4).

Our free energy reads off now as

$$A(\alpha, \beta, \gamma, \theta) = \lim_{V \rightarrow \infty} \frac{1}{V} \mathbb{E} \log \sum_{\sigma} \int \prod_{\mu}^L d\mu(z_\mu) \exp\left(\frac{\sqrt{\beta/\alpha}}{V^{1-\theta}} \sum_{i,\mu} \xi_{i,\mu} \sigma_i z_\mu\right), \quad (4.40)$$

where α accounts for the different ratio among the two parties, β the noise into the network, θ selects the graph (see Sec.(3.3)) and γ is the fine tuning inside the chosen topology.

The interpolating scheme remains the same: we introduce the right amount of random fields and use $t \in (0, 1)$ to define

$$A(t) = \frac{1}{N} \mathbb{E} \log \sum_{\sigma} \int d\mu(z_\mu) \exp[t\tilde{H}_{V,L}(\sigma, z; \xi) + (1-t)(\sum_i \tilde{a}\eta_i \sigma_i + \sum_{\mu} \tilde{b}\eta_{\mu} z_{\mu})]. \quad (4.41)$$

By performing the t -streaming easily we get

$$\partial_t A(t) = \frac{\sqrt{\beta}\gamma}{2} \langle (M - \bar{M})(N - \bar{N}) \rangle + \frac{\sqrt{\beta}\gamma}{2} \bar{M}\bar{N}, \quad (4.42)$$

⁸As we are going to see soon it is not possible to normalize the Hamiltonian -both the coupling strength and the volume extensiveness- for all the possible graphs in only one expression. We choose to normalize so to tackle immediately the better known limits, however apparent divergencies in the couplings develop and can be standardly avoided by properly rescaling the temperature corresponding to the amount of nearest neighbors, as in more classical approaches.

such that the replica symmetric sum rule gets

$$A(1) = A(0) - \frac{\sqrt{\beta}\gamma}{2}\bar{M}\bar{N}, \quad (4.43)$$

and the replica symmetric free energy reads off as

$$A(\beta, \gamma, \theta) = \log 2 + \frac{\gamma}{2V^\theta} \log \cosh(\sqrt{\beta}\bar{N}V^\theta) + \frac{\beta\gamma^2}{8}\bar{M}^2 - \frac{\sqrt{\beta}\gamma}{2}\bar{M}\bar{N}. \quad (4.44)$$

Let us now investigate some limits of this expression and its self-consistency. Note that by extremizing with respect to the order parameters we can skip \bar{N} through \bar{M} as

$$\langle \bar{N} \rangle = \frac{\sqrt{\beta}\gamma}{2} \langle \bar{M} \rangle. \quad (4.45)$$

4.5.1 $\theta = 0$ case: Fully connected, weighted and Curie-Weiss scenario

The case $\theta = 0$ reduces to a fully connected graph, and in particular in the upper bound for γ (i.e. $\gamma = 2$) its topology recovers the unweighed CW model (see sec. 3.3). We should recover here even the CW thermodynamics.

$$A(\beta, \gamma, \theta = 0) = \log 2 + \frac{\gamma}{2} \log \cosh(\beta \frac{\gamma}{2} \langle \bar{M} \rangle) - \frac{\beta\gamma^2}{8} \langle \bar{M} \rangle^2, \quad (4.46)$$

and its self-consistency relation reduces to

$$\langle \bar{M} \rangle = \tanh(\beta \frac{\gamma}{2} \langle \bar{M} \rangle).$$

This holds generally for the weighted graph; in particular when $\gamma = 2 \Rightarrow J = 1$ and the graph gets un-weighted (still fully connected), we get the standard Curie-Weiss limit once more:

$$A(\beta, \gamma = 2, \theta = 0) = \log 2 + \log \cosh(\beta \langle \bar{M} \rangle) - \beta 2 \langle \bar{M} \rangle^2, \quad (4.47)$$

$$\langle \bar{M} \rangle = \tanh(\beta \langle \bar{M} \rangle). \quad (4.48)$$

4.5.2 $\theta = 1/2$: Standard dilution and Erdos-Renyi scenario

With a scheme perfectly coherent with the previous one we can write down free energy and its coupled self-consistency as

$$A(\beta, \gamma, \theta = 1/2) = \lim_{V \rightarrow \infty} \left(\log 2 + \frac{\gamma}{2\sqrt{V}} \log \cosh\left(\frac{\beta\gamma}{2}\sqrt{V}\langle \bar{M} \rangle\right) - \frac{\beta\gamma^2}{8}\langle \bar{M} \rangle^2\right), \quad (4.49)$$

$$\langle \bar{M} \rangle = \lim_{V \rightarrow \infty} \tanh\left(\frac{\beta\gamma}{2}\sqrt{V}\langle \bar{M} \rangle\right). \quad (4.50)$$

Let us stress that, as $\sqrt{J} = \frac{\gamma}{2\sqrt{V}}$, the argument of the logarithm of the hyperbolic cosine scales as $\sqrt{JV}\langle \bar{M} \rangle$: This is coherent with the lack of a proper normalization into the Hamiltonian (4.39) because

for $\theta = 1/2$ the latter is still divided by V which should not appear. To avoid the lack of a universal normalization, we need to renormalize the local average coupling by a factor V so that we get the correct behavior, namely we write explicitly the free energy putting in evidence that $p \sim 1 - \exp(-\alpha\gamma^2/4)$:

$$A(\tilde{\beta}, \gamma, \theta = 1/2) = \log 2 + \sqrt{J} \log \cosh\left(\frac{\tilde{\beta}\sqrt{J}}{p} \langle \bar{M} \rangle\right) - \frac{\tilde{\beta}J}{2p} \langle \bar{M} \rangle^2, \quad (4.51)$$

such that, being $\tilde{\beta} = \beta p V$ [3], we can easily recover the trivial limits of the CW case when $p \rightarrow 1$ (and coherently $J \rightarrow 1$, $\tilde{\beta} \rightarrow \beta$) and of the fully disconnected network $p \rightarrow 0 \Rightarrow A(\tilde{\beta}, \gamma \rightarrow 0, \theta = 1/2) = \log 2$ as p is superlinear in γ .

4.5.3 $\theta = 1$: Extreme diluted regime

With a scheme perfectly coherent with the previous one we can write down free energy and its coupled self-consistency as

$$A(\beta, \gamma, \theta = 1) = \lim_{V \rightarrow \infty} \left(\log 2 + \frac{\gamma}{2V} \log \cosh\left(\frac{\beta\gamma}{2} V \langle \bar{M} \rangle\right) - \frac{\beta\gamma^2}{8} \langle \bar{M} \rangle^2 \right), \quad (4.52)$$

$$\langle \bar{M} \rangle = \lim_{V \rightarrow \infty} \tanh\left(\frac{\beta\gamma}{2} V \langle \bar{M} \rangle\right). \quad (4.53)$$

Of course here, with respect to the previous case, we get even stronger divergencies. Now we need to renormalize the local average coupling by a factor V^2 .

4.6 Numerics: Probability distribution

As the critical line is obtained, in the fluctuation theory, through the Gaussian ansatz, we double check our finding via numerical simulations.

First of all, we notice that since the interaction matrix J_{ij} is symmetric ($J_{ij} = J_{ji}$), detailed balance holds and it is well known [69, 4] how to introduce a Markov process for the dynamical evolution ruled by Hamiltonian (2.2) and obtain the transition rates for stationarity: Montecarlo sampling is then meaningful for equilibrium investigation.

The order parameter distribution function has been proved to be a powerful tool for studying the critical line in different kinds of systems; in particular, for magnetic systems the order parameter can be chosen as the magnetization per spin which, in finite-size systems, is a fluctuating quantity characterized by a probability distribution $P(m)$ [27]. In Ising-like models undergoing a second-order phase transition it is known that at temperatures lower than the critical temperature β_c^{-1} , the distribution $P(m)$ has a double peak, centered at the spontaneous magnetization $+m$ and $-m$. At temperatures greater than β_c^{-1} , $P(m)$ has a single peak at zero magnetization, and exactly at β_c^{-1} a double peak shape is observed.

In Fig. 4.1 we plotted numerical data for the probability distribution, obtained by means of Monte Carlo simulations, where $P(m)$ corresponds to the fraction of the total number of realizations in which the

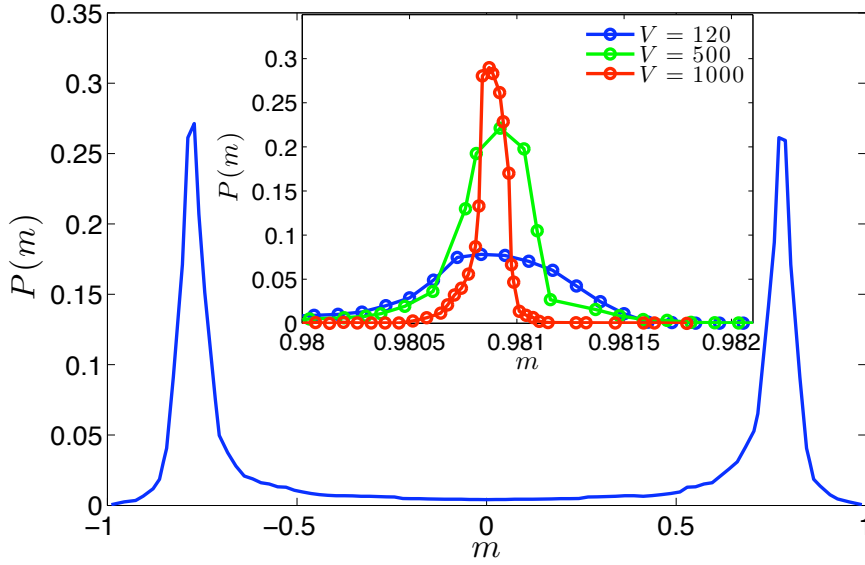


Figure 4.1: Probability distribution for the order parameter $P(m)$. Main figure: system of size $N = 1000$ at a temperature $T = 0.5T_c$; Inset: comparison between systems of size $N = 120$, $N = 500$ and $N = 1000$, as shown by the legend, set at a temperature $T = 0.9T_c$.

system magnetization is m . In the main figure we show the distribution for a system with $V = 1000$ set at a temperature $\beta^{-1} = 1.1\beta_c^{-1}$, while in the inset we compare system of different sizes set at a temperature $\beta^{-1} = 2\beta_c^{-1}$. Notice that, for such small temperatures, as the size is increased the distribution is more and more peaked, while the probability to have zero magnetization is vanishing; this corroborates the replica-symmetric ansatz.

5 Conclusion

In this paper we pioneered an alternative way for obtaining complex topologies. Interestingly from our approach small world features are emergent properties and no longer imposed a-priori, furthermore the core-theory descends from a simple shift $-1 \rightarrow 0$ in the definition domain of the patterns of an Hopfield model and is able to recover all the best known complex topologies.

From a graph theory perspective we introduced a model which, given a set of V nodes, each corresponding to a set of L attributes encoded by a binary string ξ , defines an interaction coupling $J_{ij} = (\xi_i \cdot \xi_j)$ for any couple of nodes (i, j) . The resulting system can be envisaged by means of a weighted graph displaying non trivial correlations among links. In particular, when attributes are extracted according to a discrete uniform distribution, i.e. $P(\xi_i^\mu) = (1+a)/2$ for any $i \in [1, V]$ and $\mu \in [1, L]$, being a a tunable parameter, we get that when a is sufficiently small the resulting network exhibits a small-world nature, namely a large clustering coefficient; As a is spanned, the network behaves as an isolate spin system, an extreme dilute network, a linearly diverging connectivity network a weighted fully connected and an un-weighted

fully connected network, respectively. Moreover, nodes are topologically distinguishable according to the concentration ρ of non-null entries present in their corresponding binary strings: interestingly, if the scaling among L and V is sub-linear (i.e. $P \propto \ln V$ or even slower as in low storage networks [1, 18]) the degree distribution turns out to be multi-modal, each mode pertaining to a different value of ρ . Instead, whenever the scaling is (at least) linear - $L \propto V$ -, the distribution gets mono-modal. At least numerically, at finite V, L , when looking at the distribution of weights, one finds that weak-ties work as bridge, in full agreement with Granovetter theory: indeed, one can detect small highly-connected clusters or "communities" made up of nodes with similar attributes and links connecting different communities are found to correspond a small coupling.

Then, as diluted models are of primary interest in disordered statistical mechanics, by assuming self-averaging of the order parameters, we solved the thermodynamic of the model: this required a new technique (a generalization to infinitely random fields of the double stochastic stability) which is of complete generality as well and paves another way for approaching dilution in complex systems.

Furthermore, within this framework, replicas are not necessary and instead of averaging over these copies of the system (and dealing with the corresponding overlap) we can obtain observables as magnetization averages over local subgraphs, implicitly accounting for a replica symmetric behavior (which is indeed assumed through the study).

An interesting finding, on which both the investigations converge (graph theory and statistical mechanics), is a peculiar non-mean field effect in the overall fields felt by the spins: from eq. (3.17) we see that the field insisting on a spin scales as \sqrt{J} while the averaged field on the network scales as J -see eq. (3.20)- (which is the canonical mean field expectation). Furthermore, looking at eq. (4.25) we see that in the hyperbolic tangent encoding the response of the spin to the fields, the contribution of the other spins is not weighted by J but by \sqrt{J} . As in the thermodynamics the coupling strength has been normalized, $J < 1 \rightarrow \sqrt{J} > J$: in complex thermodynamics there is a super-linearity among the interactions: despite this does not affect the critical behavior which is a global feature of the system and consequently is found to scale with J (see eq. (4.37)), this may substantially change all the other speculations based on intuition.

Of course, in the Curie-Weiss limit this effect disappear as global and local environments do coincide (i.e. $J = 1$).

It is worth stressing that (microscopic) correlation among bit-strings is directly related to macroscopic behavior (e.g. critical line), providing a new intriguing mechanics to study the former via investigations on the latter (e.g. in social networks, gene regulatory networks, or immune networks).

Next step in the research now should be double directed: from one side, a clear statistical mechanics of scale free networks may stem from our approach. From the other side, applications of this theory to real systems (first at all a clear investigation on dynamical retrieval properties), both in biology and in sociology, should be a primary challenge as well.

Acknowledgments

Francesco Guerra as usual is acknowledged for priceless scientific and human interchange.

This work is supported by the FIRB grant: *RBF08EKEV*

AB is grateful even to the Smart-Life Grant for partial support.

INFN and GNFM are acknowledged too for their partial support.

References

- [1] E. Agliari, A. Barra, *Statistical mechanics of idiotypic immune networks*, submitted to J. Theor. Bio. (2010).
- [2] E. Agliari, R. Burioni, *Random Walk on Deterministic Scale-Free networks*, Phys. Rev. E, **80**, 031125 (2009).
- [3] E. Agliari, A. Barra, F. Camboni, *Criticality in diluted ferromagnets*, J. Stat. Mech. P10003, (2008).
- [4] E. Agliari, A. Barra, R. Burioni, P. Contucci, *New perspectives in the equilibrium statistical mechanics approach to social and economic sciences*, Mathematical modeling of collective behavior in socio-economic and life sciences, Birkhauser Editor (2010).
- [5] E. Agliari, R. Burioni, D. Cassi, F.M. Neri *Autocatalytic Reactions on low-dimensional structures*, Thoe. Chem. Acc., 118, 855 (2007).
- [6] E. Agliari, A. Blumen, O. Mülken, *Dynamics of Continuous-time quantum walks in restricted geometries*, J. Phys. A, 41, 445301 (2008).
- [7] E. Agliari, M. Casartelli, A. Vezzani, *Energy transport in an Ising disordered model*, J. Stat. Mech., 07041 (2009).
- [8] E. Agliari, M. Casartelli, E. Vivo, *Metric characterization of cluster dynamics on the Sierpinski gasket*, submitted.
- [9] D. ben-Avraham, S. Havlin, *Diffusion and Reactions in Fractals and Disordered Systems*, Cambridge University Press, (2000).
- [10] D.J. Amit, *Modeling brain function: The world of attractor neural network* Cambridge University Press, (1992)
- [11] D.J. Amit, H. Gutfreund, H. Sompolinsky, *Storing infinite numbers of patterns in a spin glass model of neural networks*, Phys. Rev. Lett. **55**, (1985).
- [12] D.J. Amit, H. Gutfreund, H. Sompolinsky, *Information storage in neural networks with low levels of activity*, Phys. Rev. A **35**, (1987).
- [13] D.J. Amit, H. Gutfreund, H. Sompolinsky, *Information storage in neural networks with low levels of activity*, Phys. Rev. A **35**, (1987).
- [14] R. Albert, A. L. Barabasi *Statistical mechanics of complex networks*, Reviews of Modern Physics **74**, 47-97 (2002).
- [15] A. L. Barabasi, Z. N. Oltvai, *Network biology: understanding the cell's functional organization*, Rev. Nature Genetics **5**, 101-116, (2004).
- [16] A. Barra, *The mean field Ising model through interpolating techniques*, J. Stat. Phys. **132**, N.5, 787-809, (2008).
- [17] A. Barra, *Irreducible free energy expansion and overlap locking in mean field spin glasses*, J. Stat. Phys. **123**, N.3, 601-614, (2006).

- [18] A. Barra, E. Agliari, *Autopoietic immune networks from a statistical mechanics perspective*, J. Stat. Mech. P07004, (2010).
- [19] A. Barra, E. Agliari, *Stochastic dynamics for idiotypic immune networks*, submitted to Physica A (2010).
- [20] A. Barra, F. Camboni, P. Contucci, *Dilution robustness for mean field ferromagnets*, J. Stat. Mech. P03028, (2009).
- [21] A. Barra, P. Contucci, *Toward a quantitative approach to migrants integration*, Europhys. Lett. **89**, 68001 – 68007, (2010).
- [22] A. Barra, F. Guerra, *About the ergodicity in Hopfield analogical neural network*, J. Math. Phys. **49**, 125217, (2008).
- [23] A. Barra, F. Guerra, G. Genovese, *The replica symmetric behavior of the analogical neural network*, J. Stat. Phys. **140**, N.4, 784 – 796, (2010).
- [24] A. Barrat, M. Weigt, *On the properties of small-world network models*, Europ. Phys. J. B **13**, 547, (2000).
- [25] A. Barrat, M. Barthélemy, A. Vespignani, *Dynamical processes in complex networks*, Cambridge University Press (2008).
- [26] D. ben-Avraham, S. Havlin, *Diffusion and Reactions in Fractals and Disordered Systems*, Cambridge University Press (2000).
- [27] K. Binder, D. P. Landau, *Guide To Monte Carlo Simulations In Statistical Physics*, Cambridge University Press (2009).
- [28] C. C. F. Blake, *Do genes in pieces imply proteins in pieces?* Nature **273**, 267 (1978).
- [29] B. Bollobas, *Random graphs*, Cambridge Stud. Advanc. Math., Cambr. Univ. Press. (1985).
- [30] J.P. Bouchaud, M. Potters, *Theory of financial risks: from statistical physics to risk management*, Oxford University Press, (2004).
- [31] R. Burioni, D. Cassi, *Energy transport in an Ising disordered model*, J. Phys. A, 38, R45 (2005).
- [32] W. Brock, S. Durlauf, *Discrete choices with social interactions*, Rev. Econ. St. **68**, (2001).
- [33] M. Buchanan, *Nexus: Small Worlds and the Groundbreaking Theory of Networks*. Norton, W. W. Company, Inc. (2003).
- [34] M. Buchanan, G. Caldarelli, P. De Los Rios, F. Rao and M. Vendruscolo (eds), *M. Modelling cell biology with networks*, Cambridge Univ. Press (2010).
- [35] F.M. Burnet, *The clonal selection theory of acquired immunity*, Cambridge University Press, (1959).
- [36] D. Callaway, M.E.J. Newman, S.H. Strogats, D.J. Watts, *Network robustness and fragility: Percolation on random graphs*, Phys. Rev. Lett. **85**, 5468 (2000).
- [37] A.C.C. Coolen, R. Kuehn, P. Sollich, *Theory of Neural Information Processing Systems*, Oxford Univ. Press, (2005).

- [38] A.C.C. Coolen, S. Rabello, *Generating functional analysis of complex formation and dissociation in large protein interaction networks*, Proc. IW-SMI-2009, Kyoto, J. Phys. Conference Series, (2009).
- [39] A. Dembo, A. Montanari, *Gibbs Measures and Phase Transitions on Sparse Random Graphs*, course taught at the 2008 Brazilian School of Probability (2008).
- [40] S.N. Durlauf, *How can statistical mechanics contribute to social science?*, Proc. Natl. Ac. Sc. **96**, (1999).
- [41] R.S. Ellis, *Large deviations and statistical mechanics*, Springer, New York (1985).
- [42] C. Francke, R.J. Siezen, B. Teusink, *Reconstructing the metabolic network of a bacterium from its genome*, Trends in Microbiol. **13**, 550 – 558, (2005).
- [43] L. De Sanctis, F. Guerra, *Mean field dilute ferromagnet I. High temperature and zero temperature behavior*, J. Stat. Phys. **132**, (2008).
- [44] M. Galiceanu, A. Blumen, *Spectra of Husimi cacti: Exact results and applications*, J. Chem. Phys., **127**, 134904 (2007).
- [45] I. Gallo, A. Barra, P. Contucci, *Parameter Evaluation of a Simple Mean-Field Model of Social Interaction*, Math. Meth. & Models in Applied Sciences **19**, 1427 – 1439, (2008).
- [46] A.C. Gavin et al., *Functional organization of the yeast proteome by systematic analysis of protein complexes*, Nature **415**, 141 – 147, (2002).
- [47] G. Genovese, A. Barra, *A mechanical approach to mean field spin models*, J. Math. Phys. **50**, 053303, (2009).
- [48] G. Genovese, A. Barra, *A certain class of Curie-Weiss models*, arXiv:0906.4673, (2009).
- [49] L.H. Greene, V.A. Higman, *Uncovering network system within protein structures*, J. Molec. Bio. **334**, (2003).
- [50] F. Guerra, *Broken Replica Symmetry Bounds in the Mean Field Spin Glass Model*, Comm. Math. Phys. **233**, 1-12, (2003).
- [51] F. Guerra, *Sum rules for the free energy in the mean field spin glass model*, in *Mathematical Physics in Mathematics and Physics: Quantum and Operator Algebraic Aspects*, Fields Institute Communications **30**, Amer. Math. Soc. (2001).
- [52] M.S. Granovetter, *The Strength of Weak Ties*, Amer. J. of Sociology **78**, 1360 – 80, (1973).
- [53] M.S. Granovetter, *The Strength of the Weak Tie: Revisited*, Sociol. Theory **1**, 201 – 33, (1983).
- [54] E.L. Berlow, *Strong effects of weak interactions in ecological communities*, Letters to Nature **398**, 330 – 334, (1999).
- [55] D.O. Hebb, *Organization of Behaviour*, Wiley, New York, (1949).
- [56] J.J. Hopfield, *Neural networks and physical systems with emergent collective computational abilities*, P.N.A.S. **79**, (1982).
- [57] E. Jantsch, *The Self-Organizing Universe: Scientific and Human Implications of the Emerging Paradigm of Evolution*, Sys. Sc. World Order Libr. (1990).

- [58] N.K. Jerne, *Toward a network theory of the immune system*, Ann. Immun. **125**, (1974).
- [59] C. Martelli, A. De Martino, E. Marinari, M. Marsili, I. Perez-Castillo, *Identifying essential genes in E. coli from a metabolic optimization principle*, Proc. Natl. Acad. Sc. **106** 2607, (2009).
- [60] D. McFadden, *Economic choices*, American Econ. Rev. **91**, 351 – 378, (2001).
- [61] D. Medini, A. Covacci, and C. Donati, *Protein Homology Network Families Reveal step-wise diversification*, PLoS 2, Comp. Bio., **12**, (2006).
- [62] M. Mézard, G. Parisi and M. A. Virasoro, *Spin glass theory and beyond*, World Scientific, Singapore (1987).
- [63] S. Milgram, *The Small World Problem*, Psych. Today **2**, 60 – 67, (1967).
- [64] J. M. Montoya, R. V. Sole', *Small World Patterns in Food Webs*, J. Theor. Biol. **214**, 3, (2002).
- [65] T. Nikolettopoulos, A.C.C. Coolen, I. Perez-Castillo, N.S. Skantzos, J.P.L. Hatchett, B. Wemmenhove, *Replicated Transfer Matrix Analysis of Ising Spin Models on 'Small World' Lattices*, J. Phys. A **37**, (2004).
- [66] G. Parisi, *A simple model for the immune network*, P.N.A.S. **87**, (1990).
- [67] G. Parisi, *Statistical field theory*, Frontiers in physics, (1998).
- [68] L. Peliti, *Introduction to the statistical theory of Darwinian evolution*, Lectures at the Summer College on Frustrated System, Trieste, August (1997).
- [69] I. Perez-Castillo, B. Wemmenhove, J.P.L. Hatchett, A.C.C. Coolen, N.S. Skantzos, T. Nikolettopoulos, *Analytic Solution of Attractor Neural Networks on Scale-free Graphs*, J. Phys. A **37**, (2004).
- [70] S. Rabello, A.C.C. Coolen, C.J. Perez-Vicente and F. Fraternali, *A solvable model of the genesis of amino-acid sequences via coupled dynamics of folding and slow genetic variation*, J. Phys. A **41**, 285004, (2008).
- [71] D.J. Watts, S.H. Strogatz, *Collective dynamics of small world networks*, Nature **393**, (1998).
- [72] D.J. Watts. *An Experimental Study of Search in Global Social Networks*, Science, (2003).
- [73] Z. Füredi and J. Komlós, *The eigenvalues of random symmetric matrices*, Combinatorica **1** (1981), no. 3, 233-241
- [74] D. Achlioptas, R. M. D'Souza, J. Spenceer, *Explosive Percolation in Random Networks*, Science, **323**, 1453 (2009)
- [75] A.A. Moreira, E.A. Oliveira, S.D.S. Reis, H.J. Herrmann, J.S. Andrade Jr., *A Hamiltonian approach for explosive percolation* [archivio](#)
- [76] H.D. Rozenfeld, L.K. Gallos, H.A. Makse, *Explosive percolation in the Human Protein Homology Network* [archivio](#)
- [77] M.E.J. Newman, *The structure and function of complex networks*, SIAM Review, 45, 167-256 (2003), and references therein

- [78] R. Albert and A.-L. Barabási, *Statistical mechanics of Complex Networks*, Rev. Mod. Phys. 74, 47-98 (2002), and references therein
- [79] M. Molloy and B. Reed, *The size of the giant component of a random graph with a given degree sequence*, Combinatorics, Probability and Computing 7, 295-305 (1998)
- [80] H. Jeong, S.P. Mason, Z.N. Oltvai and A.-L. Barabási, Nature 411, 41 (2001)
- [81] M.E.J. Newman, *Assortativity Mixing in Networks*, Phys. Rev. Lett., 89, 208701 (2002)
- [82] G.R. Grimmett, *Percolation*, Springer-Verlag, Berlin 1999.
- [83] B. Bollobás, O. Riordan *Percolation*, Cambridge University Press, Cambridge 2006.
- [84] Watkin T L H and Sherrington D 1991, *Europhys. Lett.* 14, 791
- [85] B. Wemmenhove, N. S. Skantzos, A. C. C. Coolen, 2004 J. Phys. A: Math. Gen. 37, 7653
- [86] Said M R, Begley T J, Oppenheim A V, Lauffenberger D A and Samson L D 2004, *Proc. Nat. Am. Soc.* 101, 18006
- [87] Uetz P, Dong Y-A, Zeretzke C, Atzler C, Baiker A, Berger B, Rajagopala S V, Roupelieva M, Rose D, Fossum E and Haas J, 2006 Science 311, 239
- [88] E. Agliari, A. Barra, forthcoming.
- [89] Breskin I, Soriano J, Moses E and Tlusty T, 2006, *Phys. Rev. Lett.* 97, 188102